Visual Displays that Directly Interface and Provide Read-Outs of Molecular States via Molecular Graphics Processing Units**

Julia E. Poje, Tamara Kastratovic, Andrew R. Macdonald, Ana C. Guillermo, Steven E. Troetti, Omar J. Jabado, M. Leigh Fanning, Darko Stefanovic, and Joanne Macdonald

Abstract: *The monitoring of molecular systems usually requires sophisticated technologies to interpret nanoscale events into electronic-decipherable signals. We demonstrate a new method for obtaining read-outs of molecular states that uses graphics processing units made from molecular circuits. Because they are made from molecules, the units are able to directly interact with molecular systems. We developed deoxyribozyme-based graphics processing units able to monitor nucleic acids and output alphanumerical read-outs via a fluorescent display. Using this design we created a molecular 7-segment display, a molecular calculator able to add and multiply small numbers, and a molecular automaton able to diagnose Ebola and Marburg virus sequences. These molecular graphics processing units provide insight for the construction of autonomous biosensing devices, and are essential components for the development of molecular computing platforms devoid of electronics.*

Modern electronic computing systems have permeated nearly every aspect of modern life, including the molecular sciences, where our reliance on electronics ranges from simple digital data storage to sophisticated laboratory equipment. Even proponents of alternative molecular computing systems[1] are reliant on electronic devices to translate molecular events into electronic-decipherable signals. Yet the vision for molecular computing is devices that are devoid of electronics. Here we explore the implications and current limitations of an electronics-less landscape for autonomous molecular output devices. We present a platform that provides graphics processing and visual displays that operate analogously to electronic displays, but are built from biomolecules. The system employs deoxyribozyme-based molecular logic gates[2] and circuitry,[1a–e] which uses oligonucleotides as inputs and produces oligonucleotide outputs; the accumulation of output is measured by fluorescent-resonance energy transfer (FRET) tagging of the output molecule. We demonstrate a molecular 7-segment display circuit, and a molecular calculator able to add and multiply small numbers. The output is a static alphanumeric fluorescent display with utility for providing temporary read-outs of molecular states. To demonstrate the usefulness of this display for autonomous biosensors, we constructed a prototype diagnostic molecular automaton able to identify signature sequences found in Ebola and Marburg virus pathogen genomes that displays viral identity in colored fluorescent text.

Our inspiration for the development of the first molecule-based graphic processing units was the ubiquitous and simple electronic display known as the 7-segment display (Figure 1A). This display is found in many electronic devices including digital watches and elevator screens. The display energizes output lines to form decimal digits using seven different segments on a light-emitting diode (LED) display. Four-bit binary coded decimal (BCD) values are used as inputs, which are decoded for display by a BCD decoder (Figure 1B). The BCD inputs are designated A, B, C, and D, and outputs are labelled a, b, c, d, e, f, and g, where each letter corresponds to a standardized segment designation for 7-segment displays. To encode the system for deoxyribozyme-based molecular logic (Figure 1C),[1c,2a,b] we designated four input oligonucleotides to represent A, B, C and D. We then

[*] J. E. Poje, T. Kastratovic, A. C. Guillermo, S. E. Troetti, Dr. J. Macdonald
Division of Experimental Therapeutics, Department of Medicine
Columbia University
630 W 168th St, New York, NY 10032 (USA)
E-mail: jm2236@columbia.edu

Dr. J. Macdonald
Genecology Research Centre, Inflammation and Healing Research Cluster, School of Science and Engineering
University of the Sunshine Coast
Queensland (Australia)
E-mail: jmacdon1@usc.edu.au

A. R. Macdonald
Interfathom, LLC
Chicago, IL 60680 (USA)

Dr. O. J. Jabado
Department of Genetics and Genomic Sciences
Mount Sinai School of Medicine
New York, NY 10029 (USA)

M. L. Fanning, Prof. D. Stefanovic
Department of Computer Science, University of New Mexico
Albuquerque, NM 87131 (USA)

Prof. D. Stefanovic
Center for Biomedical Engineering, University of New Mexico
Albuquerque, NM 87131 (USA)

designed a circuit of deoxyribozyme-based logic gates (Figure 1D) to convert presence of the BCDs to activation of output. Unlike electronic 7-segment displays, the automaton was not designed to display the value zero in the absence of inputs, but rather mimic a biological system that traditionally would display no result in the absence of incoming signals. Similar to our previous automata,[1c,e] sufficient fluorescent accumulation allowed accurate visualization of output using an electronic plate reader after 35 min, although some individual numbers appeared as early as 10 min (Figure 1E). We also observed that fluorescence could be visualized simply by dispensing reagents in a clear-bottomed microtitre plate and viewing using a standard UV-light box, albeit after an overnight incubation. This simpler method of visualization is

a step closer to the goal of molecular computing devices that do not require batteries or wires.

To demonstrate the utility of our display format for molecular computing applications, we designed a prototype molecular calculator able to add or multiply the numbers 1, 2, and 3, and display the calculation result visually using a fluorescent 7-segment display (Figure 2A). Six oligonucleotide inputs were designated to represent the numerical calculation inputs (first input: A1–A3, second input: X1–X3), and a further two oligonucleotide inputs represented the function performed: F+ for addition and F× for multi-
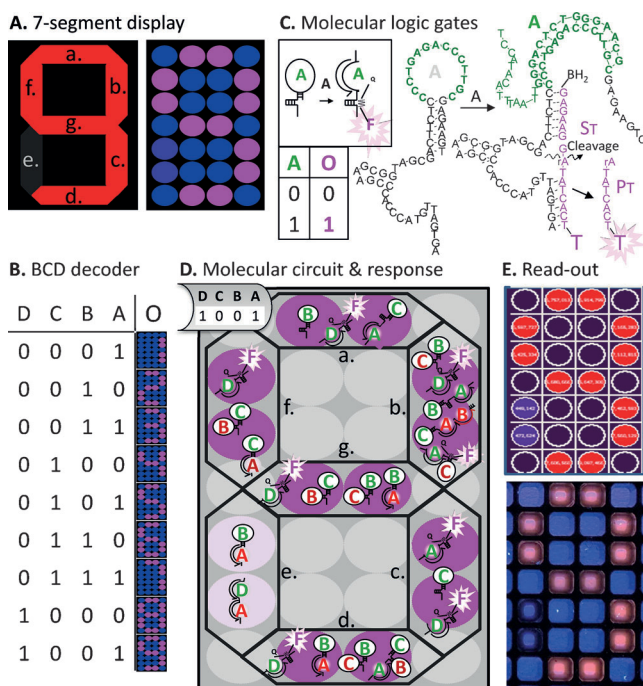

Figure 1. Molecular BCD decoder and 7-segment display. A) The traditional 7-segment display (left panel) was designed to operate in a well-plate format (right panel). B) Truth table of BCD decoder: addition of binary coded oligonucleotide inputs (A–D) produces a fluorescent decimal display output (O). C) Circuits are powered using deoxyribozyme-based molecular logic gates:[1c,2b] the YES$_A$ gate pictured is activated by addition of oligonucleotide input A, allowing cleavage of a FRET-labelled oligonucleotide substrate, producing product P$_T$ and causing the accumulation of TAMRA (T) fluorescence; additional logic gates are described in the Supporting Information, Figure S1. D) The molecular circuit for the BCD decoder and display and experimental details are described in the Supporting Information; the response of the circuit to addition of inputs A and D (1001 = 9) is shown: green letters designate activating gate segments and red letters designate inhibitor gate segments; wells producing fluorescence are highlighted in pink. E) Experimental results: oligonucleotides A and D representing the binary digit (1001) were added to every segment of the circuit and output fluorescence was visualized using a standard fluorescent plate reader (top panel) after 35 min, or color-photographed on a UV-light box after overnight incubation (bottom panel); the decimal decoded value of 9 was successfully displayed. Results for all decoded binary values are shown in Figure S2.
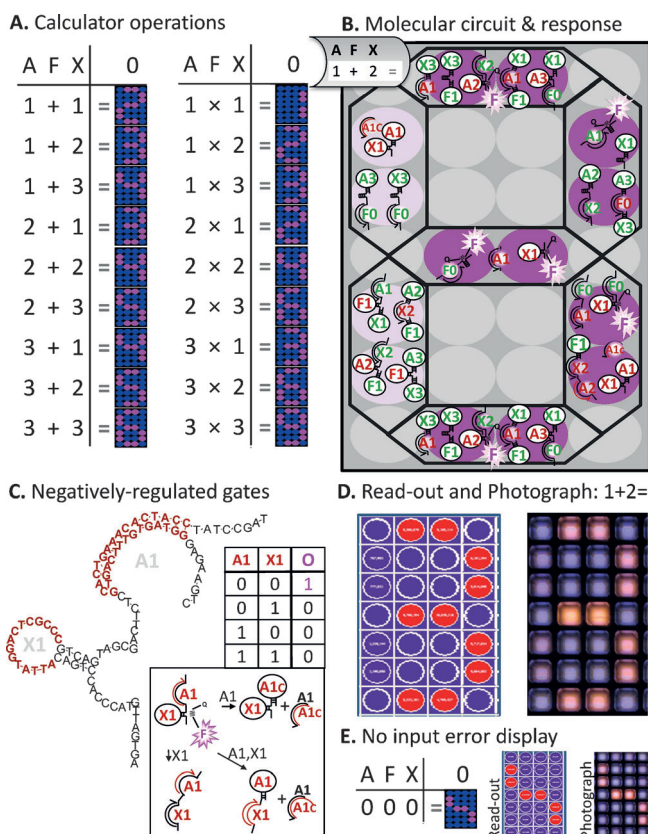
Figure 2. Molecular calculator. A) Addition of decimal coded oligonucleotide inputs (A1–A3, X1–X3), along with function-coded oligonucleotide inputs (F+ and F×) produces a fluorescent decimal display output (O). B) The circuit for the molecular calculator and experimental details are outlined in the Supporting Information; the response of the circuit to addition of inputs A1, F+, and X2 (1+2=3) is shown: green letters designate activating gate segments and red letters designate inhibitor gate segments; wells producing fluorescence are highlighted in pink. C) Negatively regulated logic gates ¬A1¬X1 (pictured) and ¬A1 (Figure S3) are constitutively active, able to cleave substrate to make product in the absence of inputs; input addition inhibits gate activity. D) Oligonucleotides A1, F+, and X2 representing the calculation 1+2 were added to every segment of the circuit; output fluorescence was visualized by fluorescent spectroscopy (left) and color photography on a UV-light box (right) after 90 min incubation at room temperature; the calculation result of 3 was successfully displayed; results for all calculations are shown in Figure S5A and B. E) The presence of constitutively active negatively regulated gates results in output production in the absence of input, producing a characteristic fluorescent pattern to be interpreted as an error symbol.

plication. The circuit required for calculator operation (Figure 2B) used similar molecular logic gates as outlined for the BCD decoder (Figure 1C), as well as two negatively regulated gate types not previously reported for any deoxyribozyme-based automata (Figure 2C). These negatively regulated gates generated fluorescence in the absence of any input, giving a characteristic reaction to be interpreted as an error signal by the user (Figure 2D). During experimental implementation we attempted to optimize the concentration of reagents for faster reaction times via UV-light-box visualization, increasing the logic gates by 10-fold, inputs by 5-fold, and substrates by 3-fold. As previously observed for our full adder automaton, simply increasing concentrations did not straightforwardly improve reaction times, confirming our earlier observation that a current limitation of the technology is defined by the total concentration of an increasing number of gates.[1c,e] To circumvent this we carefully titrated individual gate concentrations, and introduced a quenching oligonucleotide. The quenching oligonucleotide binds to product and provides a chemical threshold of product accumulation for gates to surpass before signal can be observed (see Supporting Information, Figure S4). The resultant conditions allowed clear observation of displays within 90 min of input addition (Figure 2E), representing a 16-fold improvement in speed compared with the unoptimized BCD decoders above. While the reported reaction times are exceptionally slow compared with split-second dynamic electronic displays, it should be noted that these static displays do not readily dissipate. Results remain available for viewing at least 24 hours after input addition without the requirement for ongoing electrical feeds.

A single-use static read-out that appears in 15–90 min has utility in the development of autonomous biosensors, and in particular diagnostic devices. Indeed, a system that identifies nucleic acid identity using a text display, without further processing of results, is unique. To demonstrate, we encoded a molecular automaton able to distinguish between two 15-nucleotide (nt) signature sequences found in the filovirus pathogens Ebola and Marbug virus genomes (Figure 3A). For this circuit we implemented a two-color 5×3 dot-matrix readout using both TAMRA (pink) and fluorescein (green) fluorescence colors,[1c,e] demonstrating ability to produce displays using multiple colors and layouts (Figure 3B and C). Additionally, the use of 15 wells in a dot-matrix display increases the robustness of the assay, since 15 individualized reactions are required to give a correct answer before diagnosis can be achieved. Sequences were identified using custom-designed software to scan viral genomes for 15-nt regions suitable for incorporation into logic gates.[3] The codes identified demonstrated the power of logic gates to include and exclude by design: a 15-nt code found in all filoviruses (F) identified presence of Ebola if a second 15-nt code found only in Marburg virus (M) was not present, via an F¬M (F ANDNOT M) gate (Figure 3B). The resultant prototype filovirus diagnostic automaton successfully displayed a pink "E" for Ebola and a green "M" for Marburg virus upon addition of respective 15-nt input codes (Figure 3D). A second automaton able to discriminate between signature sequences of West Nile, St Louis encephalitis and Yellow
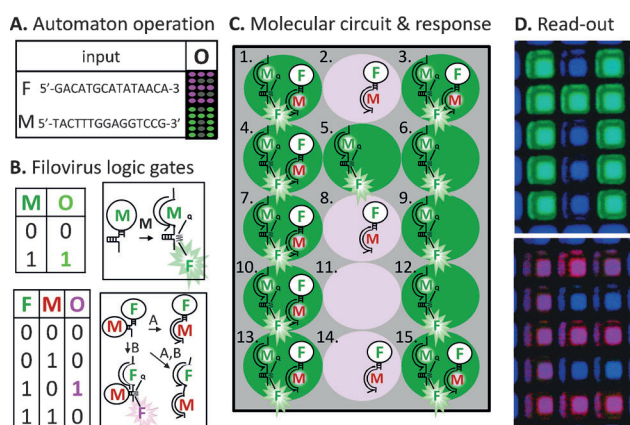
Figure 3. Diagnostic filovirus automaton. A) A diagnostic molecular circuit was designed to produce 5×3 dot-matrix text displays showing the letters E and M for Ebola and Marburg viruses, respectively, upon addition Filovirus (F) and Marburg virus (M) signature sequences. B) Two-color logic gates using both TAMRA (pink) and fluorescein (green) fluorescence colors were used,[1c,e] with a YES$_M$ gate (top) producing fluorescein (green) fluorescence, and an F¬M gate (bottom) producing TAMRA (pink) fluorescence. C) The circuit for the filovirus automaton and experimental conditions are shown in the Supporting Information; the response of the circuit to the addition of 15-nt code M is shown: green letters designate activating gate segments and red letters designate inhibitor gate segments; wells producing fluorescence are highlighted in green. D) A green M (for Marburg virus; top) was successfully displayed upon addition of 15-nt signature sequences M to every well of the automaton; similarly a pink E (for Ebola virus; bottom) was displayed upon addition of F; fluorescence plate reader results (not shown) indicated E and M appearance after 30 and 100 min of input addition respectively. Color photograph (shown) from UV-light-box visualization was taken after overnight incubation at room temperature.

Fever virus was similarly constructed (Figure S6).[4] The incorporation of viral pathogen sequences demonstrates the modularity of our logic gate design. The system is very convenient, since the fluorescent reactions occur autonomously after input addition. It is also inherently scalable as additional text can be added by simply increasing the number of wells. A two-color 15-well output system can analyse DNA mixtures to produce $2^{30} = 1\,073\,741\,824$ different patterns, providing more capability than current diagnostic possibilities. By restricting the number of patterns to meaningful text, we provide a capacity for autonomous diagnostic readout without the requirement to decipher complicated patterns of dots. Importantly, this ability to perform computation, of virtually any complexity, within each well provides a fundamental advance beyond traditional diagnostics. We provide potential to interrogate the presence, absence, or thresholding of multiple markers, and combine these inputs into clinically relevant outputs, without the need for extrinsic devices, computers, or software.

Our experiments demonstrate the first non-electronic based graphics processing units and visual displays able to interact directly with molecules and nanoscale systems. Our first-in-class molecular 7-segment display, molecular calculator and autonomous molecular diagnostic, present a new path forward in the development of "intelligent" biosensors. The

systems provide potential to analyse and condense complex sets of molecular information for efficient information transfer and dissemination. The simple reaction requirements, and novel conversion of molecular information into a visual form, confer significant benefits to the assayist, particularly as the complexity of the information increases. While currently restricted to static displays, we are developing a reset function to enable dynamic data read-out. In the short-term the displays are necessarily photographed and converted to electronic digital forms for long-term storage. However, ultimately they provide a read-out potential for molecular data storage devices. For instance, in the reported DNA-encoding of Shakespeare's sonnets,[5] read-out occurred via sophisticated high-throughput sequencing technology after 15.6 days. Development of molecular-based graphics processing units for this technology could potentially reduce read-out time to less than two hours in low-resource settings. In addition, 7-segment or dot-matrix style displays are relevant in molecular cryptographic applications:[6] rather than providing pre-set images for subsequent deciphering, our system displays sets of text or images dependent on input mixtures provided. Our graphics processing units and visual displays thus provide another component to the molecular toolkit now available, including molecular logic gates,[1c,f,h,2b,c] automata,[1b–e,i–n] storage,[5] and cryptography,[6] allowing the engineering of systems on the nano-scale that are analogous to, but devoid of, electronic components.

[1] a) M. N. Stojanović, D. Stefanović, *Nat. Biotechnol.* **2003**, *21*, 1069–1074; b) M. N. Stojanović, D. Stefanović, *J. Am. Chem. Soc.* **2003**, *125*, 6673–6676; c) H. Lederman, J. Macdonald, D. Stefanović, M. N. Stojanović, *Biochemistry* **2006**, *45*, 1194–1199; d) R. Pei, E. Matamoros, M. Liu, D. Stefanović, M. N. Stojanović, *Nat. Nanotechnol.* **2010**, *5*, 773–777; e) J. Macdonald, Y. Li, M. Sutovic, H. Lederman, K. Pendri, W. Lu, B. L. Andrews, D. Stefanović, M. N. Stojanović, *Nano Lett.* **2006**, *6*, 2598–2603; f) Z. Xie, S. J. Liu, L. Bleris, Y. Benenson, *Nucleic Acids Res.* **2010**, *38*, 2692–2701; g) D. Y. Duose, R. M. Schweller, W. N. Hittelman, M. R. Diehl, *Bioconjugate Chem.* **2010**, *21*, 2327–2331; h) G. Seelig, D. Soloveichik, D. Y. Zhang, E. Winfree, *Science* **2006**, *314*, 1585–1588; i) L. Qian, E. Winfree, *Science* **2011**, *332*, 1196–1201; j) C. C. Santini, J. Bath, A. J. Turberfield, A. M. Tyrrell, *Int. J. Mol. Sci.* **2012**, *13*, 5125–5137; k) K. Rinaudo, L. Bleris, R. Maddamsetti, S. Subramanian, R. Weiss, Y. Benenson, *Nat. Biotechnol.* **2007**, *25*, 795–801; l) T. S. Moon, C. B. Lou, A. Tamsir, B. C. Stanton, C. A. Voigt, *Nature* **2012**, *491*, 249–253; m) L. Qian, E. Winfree, J. Bruck, *Nature* **2011**, *475*, 368–372; n) S. Auslander, D. Auslander, M. Muller, M. Wieland, M. Fussenegger, *Nature* **2012**, *487*, 123; o) J. Elbaz, O. Lioubashevski, F. Wang, F. Remacle, R. D. Levine, I. Willner, *Nat. Nanotechnol.* **2010**, *5*, 417–422; p) E. Katz, V. Privman, *Chem. Soc. Rev.* **2010**, *39*, 1835–1857.

[2] a) J. Macdonald, D. Stefanovic, M. N. Stojanovic in *Fluorescent Energy Transfer Nucleic Acid Probes: Designs and Protocols*, Vol. 335 (Ed.: V. V. Didenko), Humana Press, Totowa, **2006**, pp. 343–363; b) M. N. Stojanovic, T. E. Mitchell, D. Stefanovic, *J. Am. Chem. Soc.* **2002**, *124*, 3555–3561; c) M. N. Stojanovic, S. Semova, D. Kolpashchikov, J. Macdonald, C. Morgan, D. Stefanovic, *J. Am. Chem. Soc.* **2005**, *127*, 6914–6915.

[3] a) J. E. Stajich, D. Block, K. Boulez, S. E. Brenner, S. A. Chervitz, C. Dagdigian, G. Fuellen, J. G. Gilbert, I. Korf, H. Lapp, H. Lehvaslaiho, C. Matsalla, C. J. Mungall, B. I. Osborne, M. R. Pocock, P. Schattner, M. Senger, L. D. Stein, E. Stupka, M. D. Wilkinson, E. Birney, *Genome Res.* **2002**, *12*, 1611–1618; b) M. Andronescu, R. Aguirre-Hernandez, A. Condon, H. H. Hoos, *Nucleic Acids Res.* **2003**, *31*, 3416–3422; c) P. Rice, I. Longden, A. Bleasby, *Trends Genet.* **2000**, *16*, 276–277; d) M. L. Fanning, J. Macdonald, D. Stefanovic, *DNA 15* **2009**, *LNCS 5877*, 45–54; e) J. N. Zadeh, C. D. Steenberg, J. S. Bois, B. R. Wolfe, M. B. Pierce, A. R. Khan, R. M. Dirks, N. A. Pierce, *J. Comput. Chem.* **2011**, *32*, 170–173.

[4] J. Macdonald, M. Poidinger, J. S. Mackenzie, R. C. Russell, S. Doggett, A. K. Broom, D. Phillips, J. Potamski, G. Gard, P. Whelan, R. Weir, P. R. Young, D. Gendle, S. Maher, R. T. Barnard, R. A. Hall, *Evol. Bioinf. Online* **2010**, *6*, 91–96.

[5] N. Goldman, P. Bertone, S. Chen, C. Dessimoz, E. M. LeProust, B. Sipos, E. Birney, *Nature* **2013**, *494*, 77–80.

[6] a) S. Shoshani, R. Piran, Y. Arava, E. Keinan, *Angew. Chem.* **2012**, *124*, 2937–2941; *Angew. Chem. Int. Ed.* **2012**, *51*, 2883–2887; b) C. T. Clelland, V. Risca, C. Bancroft, *Nature* **1999**, *399*, 533–534; c) K. W. Kim, V. Bocharova, J. Halamek, M. K. Oh, E. Katz, *Biotechnol. Bioeng.* **2011**, *108*, 1100–1107.